Adsorption Behavior of Malachite Green on Activated Carbon–MnO_2 Nanocomposite

R. Jothimani[1], Dr. M. Santhi[2]
[1]*Department of Chemistry, Gobi Arts & science College, Gobichettipalayam-638453, Tamil nadu, India.*
[2]*Department of Chemistry, Erode Arts and science College, Gobichettipalayam-638 009, Tamil nadu, India*

***Abstract*—The present study explores the synthesis, characterization, and adsorption efficiency of AC-MnO_2 nanocomposites for Malachite Green (MG) removal. Activated carbon from Corallocarpus epigaeus was thermally treated and combined with MnO_2 nanoparticles. Characterization via FESEM-EDX and FTIR confirmed porous morphology, MnO_2 dispersion, and functional groups. Adsorption studies showed optimal MG removal (88%) at 20 ppm, with increased adsorbent dosage enhancing efficiency until saturation. Temperature effects confirmed endothermic behavior, peaking at 98.6% at 60°C. Co-ion interactions influenced adsorption, with $(NH_4)_2CO_3$ enhancing (95.95%) and NH_4Cl reducing (33.04%) efficiency. AC-MnO_2 nanocomposites demonstrate strong potential for wastewater treatment.**

***Index Terms*—AC-MnO_2, adsorption, Malachite Green.**

I. INTRODUCTION

Water pollution caused by synthetic dyes is a major environmental challenge, particularly in industrial wastewater from textile, leather, paper, and food industries [1]. Malachite Green (MG), a triphenylmethane dye, is widely used in aquaculture and fabric dyeing but is highly toxic, carcinogenic, and resistant to biodegradation. Its persistence in aquatic environments poses serious ecological and health risks, including mutagenicity, teratogenicity, and bioaccumulation in living organisms [2]. Conventional wastewater treatment methods, such as coagulation, membrane filtration are often limited by high operational costs, incomplete removal, and secondary pollution. Hence, developing efficient, cost-effective, and sustainable removal techniques is crucial [3,4].

Adsorption has emerged as a promising technique for removing MG from aqueous solutions due to its simplicity, high efficiency, and ability to eliminate pollutants without generating harmful byproducts. Adsorbents such as activated carbon (AC), metal oxides, and their composites have been widely explored for water purification applications [5,6]. Among metal oxides, manganese dioxide (MnO_2) exhibits unique physicochemical properties, including a high surface area, variable oxidation states, strong redox potential, and excellent adsorption capacity for organic pollutants [7]. MnO_2 can effectively interact with dye molecules through electrostatic attraction, ion exchange, and oxidative degradation, making it a potential adsorbent for MG removal. However, the standalone use of MnO_2 is often restricted by its low surface area, poor mechanical stability, and aggregation tendencies, which limit its adsorption performance.

To address these limitations, hybrid materials combining AC and MnO_2 have been developed to enhance the efficiency of adsorption-based water treatment. Activated carbon is widely recognized for its exceptionally high porosity, large specific surface area, and superior adsorption capacity due to its well-developed microporous and mesoporous structures. It provides abundant active sites for dye adsorption via physical interactions, including van der Waals forces and π-π stacking, as well as chemical interactions such as hydrogen bonding and electrostatic attraction. When combined with MnO_2, AC not only prevents the aggregation of MnO_2 nanoparticles but also enhances adsorption through synergistic interactions, leading to improved dye removal efficiency. The AC–MnO_2 nanocomposite thus exhibits a unique combination of high adsorption capacity, increased surface reactivity, and enhanced stability, making it a promising candidate for water treatment applications.

This study focuses on investigating the adsorption behavior of Malachite Green on an AC–MnO_2 nanocomposite, evaluating key parameters such as temperature of reaction, concentration of MG.

II. MATERIALS & METHODS

A. Nanocomposite (adsorbent) Synthesis

Activated carbon was prepared from Corallocarpus epigaeus by drying, pulverizing, and treating the powdered material with concentrated H_2SO_4 (1:2 ratio) for 48 hours. The resulting char was washed to neutral pH, dried, and subjected to thermal activation at 700°C in a muffle furnace for one hour. For nanocomposite synthesis, 3g of activated carbon was swelled in 15 ml of anhydrous alcohol and stirred at 25°C for 2 hours. Simultaneously, 3g of manganese dioxide was dispersed in 15 ml of anhydrous alcohol, then gradually added to the activated carbon suspension and stirred for an additional 5 hours. A mixture of 5 ml alcohol and 2 ml deionized water was then introduced, followed by continuous stirring for another 5 hours. The final suspension was dried in a vacuum oven at 80°C for 6 hours to obtain the nanocomposite adsorbent.

B. Absorbate solution

Malachite Green (MG), a basic dye with the molecular formula $C_{23}H_{25}ClN_2$ and a molecular weight of 364.92 g/mol, was used as the adsorbate in this study. The dye concentration in the supernatant solution was determined using a UV-visible spectrophotometer at its characteristic maximum absorption wavelength (λmax = 617 nm). A stock solution was prepared by dissolving 1 g of MG in 1000 mL of deionized water. From this stock solution, working standard solutions of varying concentrations (10 ppm, 20 ppm, 30 ppm, and 40 ppm) were prepared in 100 mL volumetric flasks for further adsorption studies.

C. Characterization analysis

The samples were characterized using Field Emission Scanning Electron Microscopy (FESEM) coupled with Energy Dispersive X-ray Spectroscopy (EDX) on a SIGMA HV (Carl Zeiss) instrument with a Bruker Quantax 200 - Z10 EDS detector. Samples were gold-coated to avoid charging effects, and high-resolution micrographs were taken to examine surface morphology. Elemental composition was analyzed using EDX, determining the weight percentages of key elements. Functional group analysis was performed using Fourier Transform Infrared Spectroscopy (FTIR) in ATR mode with a PerkinElmer Spectrum Two spectrometer, recording spectra in the range of 4000–400 cm^{-1} to identify molecular vibrations and confirm chemical composition.

D. Experimental

The batch adsorption experiments were conducted using a series of 250 mL Erlenmeyer flasks containing a specified mass of adsorbent and 50 mL of malachite green (MG) solution at varying initial concentrations. The flasks were placed in an isothermal water-bath shaker and agitated at 100 rpm and 30°C until equilibrium was attained. Following decantation and filtration, the equilibrium dye concentrations in the solution were determined spectrophotometrically at 617 nm using a UV-visible spectrophotometer [8]. The amount of dye adsorbed and the percentage removal of MG were subsequently calculated using the appropriate adsorption equations.

$$\% \text{ Removal} = (Ci - Ce/ Ci) \times 100$$

III. RESULTS AND DISCUSSION

A. Characterisation analysis of synthesised sample

Morphological analysis

The morphology and elemental composition of activated carbon-mediated MnO2 nanocomposites (AC- MnO2NCs) were studied using Field Emission Scanning Electron Microscopy (FESEM) and Energy Dispersive X-ray Spectroscopy (EDX) (Figure 1). These analyses provide insights into the surface structure, particle distribution, and chemical makeup, all of which are critical for understanding their potential applications in catalysis.

The FESEM images, presented in Figures 1 a and b, show the surface morphology of the AC- MnO2NCs at different magnifications. At 6.03 KX magnifications (Figure 1a), the nanocomposites exhibit irregular and rough surfaces, with noticeable agglomeration. This porous, uneven texture is characteristic of activated carbon, known for its high surface area, which enhances catalytic efficiency. The MnO2 nanoparticles are embedded in the carbon matrix, appearing as smaller granules attached to the rough carbon surfaces. The agglomeration of nanoparticles suggests strong intermolecular interactions, likely a result of van der Waals forces during synthesis, though the carbon matrix helps stabilize the dispersion of MnO2 NCs [9,10].

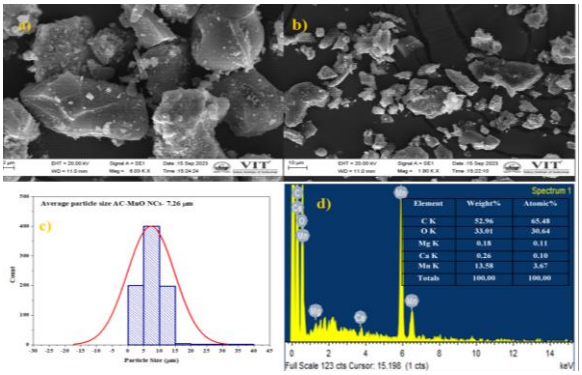

Figure 1FESEM-EDX analysis of AC-MnO2 NCs: (a,b) FESEM of AC-MnO2 Ncs (c) Particle size histograms (d) EDX analysis

At a lower magnification (1.90 KX, Figure 1b), the FESEM image reveals the overall particle distribution, with larger clusters of aggregated particles. This agglomeration is expected in nanocomposite materials, where particles tend to coalesce during synthesis. Despite the aggregation, the activated carbon support helps maintain structural integrity and sufficient surface area for effective catalytic performance [11]. The interconnected porous network of the carbon matrix also supports the dispersion of MnO2nanoparticles, enhancing their interaction with substrates during catalysis. The presence of pores between the particles is crucial, as it allows for better interaction with reactants, particularly in environmental applications where the degradation of pollutants requires high surface accessibility.

The particle size distribution, shown in Figure 1c, indicates an average particle size of 7.26 µm, reflecting the aggregated nature of the composite rather than individual nanoparticles. Although larger particle sizes typically reduce the surface area, the porous carbon matrix compensates for this by offering a significant amount of surface exposure. The relatively narrow size distribution suggests uniformity in synthesis, despite the larger aggregate size.

EDX analysis (Figure 1d) confirms the elemental composition of the AC- MnO2 nano composites. The predominant elements detected were carbon (C), oxygen (O), and manganese (Mn), with trace amounts of calcium (Ca) and magnesium (Mg). The carbon content was the highest, comprising 52.96% by weight and 65.48% by atomic percentage. This high carbon concentration is consistent with the use of activated carbon as the primary matrix. The significant oxygen content, at 33.01% by weight and 30.64% by atomic percentage, is attributed to both the oxygen-containing functional groups on the activated carbon surface and the manganese oxide structure [12,13].

Manganese was present at 13.58% by weight and 3.67% by atomic percentage, confirming the successful incorporation of MnO2 nanoparticles into the composite. The relatively low atomic percentage of manganese, compared to carbon and oxygen, suggests that the MnO2 nanoparticles are well-dispersed within the carbon matrix, which is important for maintaining stability while providing active sites for catalytic reactions.

Trace amounts of calcium (0.26%) and magnesium (0.18%) were also detected. These elements likely originate from impurities during synthesis or from the raw materials used in the process. Although present in small quantities, these elements can influence the overall properties of the nanocomposite, potentially affecting its mechanical stability or offering minor catalytic contributions.

In summary, FESEM-EDX analysis provides a detailed understanding of the AC- MnO2 nanocomposites' structural and compositional characteristics. The rough, porous morphology observed in the FESEM images is typical of activated carbon, which supports the dispersion of MnO2 nanoparticles while maintaining high surface area and stability. EDX analysis confirms the presence of manganese oxide, carbon, and oxygen, which are critical for the nanocomposites' catalytic properties. Although the particles exhibit some aggregation, the porous carbon matrix compensates for the larger particle size by offering sufficient surface area for adsorption and catalytic processes. The combination of MnO2's redox activity and the high surface area of activated carbon make this nanocomposite a promising material for environmental applications, particularly in the removal of organic pollutants.

Functional group analysis

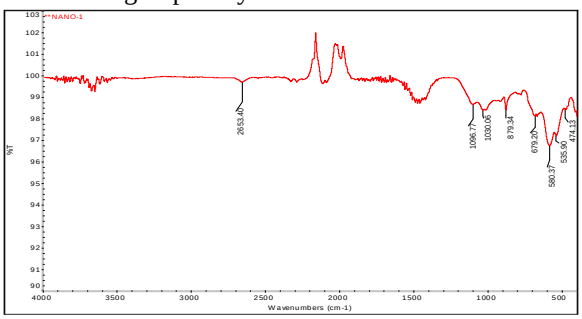

Figure 2 FTIR analysis of synthesized sample

The FTIR analysis of activated carbon doped with MnO_2 revealed characteristic peaks corresponding to both the functional groups of activated carbon and the structural Mn-O bonds of α-MnO_2. The peak at 2653 cm^{-1} suggests the presence of O-H stretching vibrations, likely from adsorbed water or hydroxyl functional groups [13]. The peaks observed at 1096 cm^{-1} and 1030 cm^{-1} correspond to C-O stretching vibrations, indicating oxygen-containing functional groups on the carbon surface [14]. Additionally, the peak at 876 cm^{-1} may be attributed to C-H bending vibrations or surface interactions involving Mn-O. The presence of α-MnO_2 was confirmed by the distinct peaks at 535 cm^{-1} and 474 cm^{-1}, with the strong peak at 535 cm^{-1} specifically attributed to Mn-O bond vibrations [15]. These findings confirm the successful incorporation of MnO_2 into the activated carbon matrix, with the observed functional groups suggesting potential improvements in adsorption capacity and catalytic activity.

B. Batch Adsorption Experiments

Effect of Initial MG Concentration on Adsorption Efficiency

The adsorption efficiency of Malachite Green (MG) onto the catalyst was evaluated at varying initial concentrations (10–40 ppm) under controlled conditions: 100 mg of AC-MnO_2-NC in 50 mL of solution at 30°C in 180 minutes. The results demonstrate a clear relationship between MG concentration and adsorption efficiency. At 10 ppm, the adsorption efficiency was 82%, increasing to a maximum of 88% at 20 ppm. However, as the concentration further increased to 30 ppm and 40 ppm, the efficiency slightly decreased to 87% and 85%, respectively. This trend suggests that at lower concentrations, the catalyst provides sufficient active sites for MG adsorption, leading to high removal efficiency. The peak efficiency observed at 20 ppm indicates optimal adsorption conditions. Beyond this concentration, the decline in efficiency may be attributed to the progressive saturation of available adsorption sites, reducing the catalyst's ability to capture additional MG molecules [16]. Overall, the adsorption process is highly effective at lower MG concentrations, with maximum efficiency at 20 ppm. At higher concentrations, reduced efficiency suggests potential limitations in active site availability and adsorption capacity.

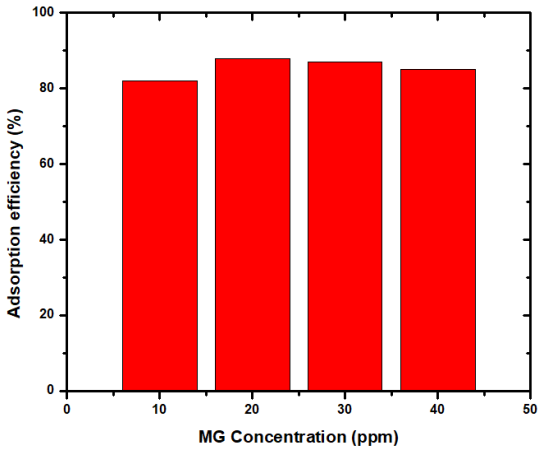

Figure 3 Effect of Initial MG Concentration on Adsorption Efficiency

Effect of Catalyst Dosage on MG Adsorption Efficiency

The adsorption efficiency of Malachite Green (MG) was evaluated as a function of AC-MnO_2-NC catalyst dosage at a fixed MG concentration of 40 ppm, a contact time of 90 minutes, and a temperature of 30°C. The results indicate a strong dependence of MG removal efficiency on the catalyst amount. At lower catalyst dosages (0.01–0.03 g), the removal efficiency was minimal, ranging from 1.37% to 4.08%, due to insufficient active adsorption sites. A notable increase in efficiency was observed at 0.04 g (24.81%) and 0.05 g (26.45%), suggesting improved MG adsorption as more active sites became available. As the catalyst dosage further increased, the removal efficiency continued to rise, reaching 44.00% at 0.06 g and 55.22% at 0.07 g. The highest adsorption efficiency of 74.33% was achieved at 0.1 g, indicating the optimal dosage for maximum MG removal. The increasing adsorption efficiency with higher catalyst dosage is attributed to the greater availability of active sites, facilitating more MG uptake. However, beyond 0.07 g, the rate of efficiency improvement slowed, likely due to adsorption site saturation or particle aggregation, which may reduce the effective surface area [17]. These results suggest that while increasing catalyst dosage enhances MG removal, the highest efficiency is achieved at 0.1 g. Therefore, selecting an optimal dosage is crucial for maximizing adsorption performance while maintaining cost-effectiveness.

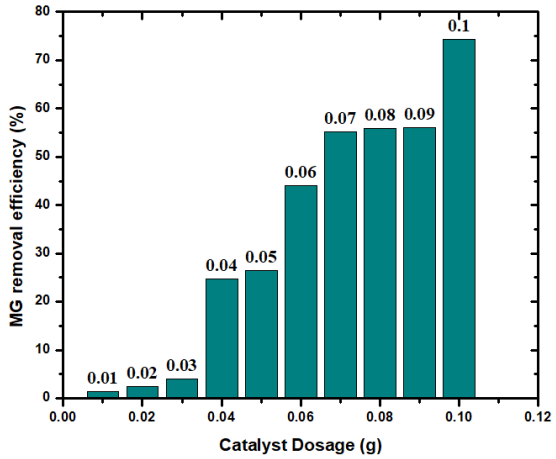

Figure 4 Effect of catalyst dosage on Adsorption Efficiency

Effect of Temperature

The effect of temperature on the adsorption of Malachite Green (MG) using AC-MnO_2-NC (100 mg/50 mL) as a catalyst was investigated by analyzing adsorption efficiency at different concentrations and temperatures, with a reaction time of 180 minutes.The study aimed to understand the thermodynamic nature of the adsorption process and its implications for dye removal efficiency. Experimental data revealed that adsorption efficiency increased with temperature, suggesting an endothermic adsorption mechanism. At 30°C, adsorption efficiency varied significantly with MG concentration, reaching 82% at 10 ppm and 85% at 40 ppm. The efficiency was lower at 40°C, particularly at 20 ppm, where it dropped to 36%, indicating a potential energy barrier to adsorption at this temperature. However, at 50°C and 60°C, adsorption efficiency remained consistently high across all concentrations, with maximum values of 91.3% and 98.6% at 30 ppm, respectively. The increasing efficiency at elevated temperatures indicates enhanced molecular interactions between MG molecules and the MnO_2 surface.

The observed trend suggests that higher temperatures facilitate the adsorption process by increasing the mobility of MG molecules and promoting stronger interactions with active sites on the MnO_2 catalyst. The adsorption process likely involves physical and chemical interactions, where temperature enhances diffusion rates and possibly influences surface reaction kinetics [18,19,20]. The significant increase in efficiency at 60°C supports the hypothesis that the adsorption mechanism follows an endothermic pathway, with temperature playing a crucial role in overcoming activation energy barriers.

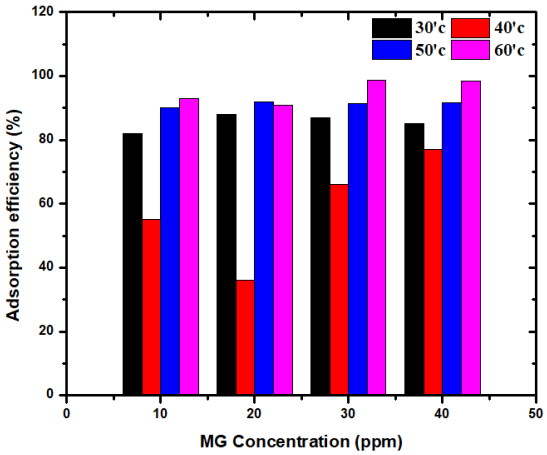

Figure 5 Effect of reaction temperature on Adsorption Efficiency

Effect of ion on adsorption process

The effect of co-ions on the adsorption of malachite green (MG) by AC-MnO_2-NC was evaluated at a concentration of 40 mg/L of dye and an adsorbent dosage of 2%. The addition of various salt solutions, including $BaCl_2$, KCl, NH_4Cl, $(NH_4)_2CO_3$, and NaCl, significantly impacted the adsorption efficiency (table 1). The removal efficiency of MG in the presence of these salts varied, with ammonium carbonate ($(NH_4)_2CO_3$) exhibiting the highest removal efficiency at 95.95%, followed by potassium chloride (KCl) at 90.74%. Barium chloride ($BaCl_2$) and sodium chloride (NaCl) demonstrated moderate effects, resulting in removal efficiencies of 68.88% and 84.59%, respectively. In contrast, ammonium chloride (NH_4Cl) showed the least effect on adsorption, with a removal efficiency of only 33.04%. These results suggest that the presence of specific ions can either enhance or reduce the adsorption process depending on their interaction with the dye molecules. The higher removal efficiency observed with ammonium carbonate could be attributed to the specific chemical interactions between the ammonium ions and the dye, promoting greater adsorption. Conversely, ammonium chloride likely interferes with the adsorption due to the competition between ammonium ions and dye molecules. Potassium chloride and sodium chloride, being simpler salts, also affected the adsorption process, albeit to a lesser extent. Overall, the ionic species played a critical role in modulating the adsorption capacity of AC-MnO_2-NC, with variations

in removal efficiency linked to ion-specific interactions and their influence on the surface properties of the adsorbent.

Table 1: Effect of co ion on adsorption process

Effect of Co-ions	Removal Efficiency (%)
$BaCl_2$	68.88
KCl	90.74
NH_4Cl	33.04
$(NH_4)_2CO_3$	95.95
NaCl	84.59

IV. CONCLUSION

This study successfully synthesized and characterized an activated carbon-manganese dioxide (AC-MnO_2) nanocomposite and demonstrated its potential as an efficient adsorbent for Malachite Green (MG) dye removal from aqueous solutions. The FESEM-EDX and FTIR analyses confirmed the successful incorporation of MnO_2 nanoparticles into the porous activated carbon matrix, providing high surface area and stability. Batch adsorption experiments revealed that adsorption efficiency was strongly influenced by initial dye concentration, catalyst dosage, temperature, and co-ion presence. The optimal adsorption conditions were observed at 20 ppm MG concentration and 0.1 g of adsorbent, achieving a maximum efficiency of 88%. Temperature-dependent studies indicated an endothermic adsorption mechanism, with efficiency reaching 98.6% at 60°C. The presence of co-ions had a variable impact, with ammonium carbonate enhancing adsorption while ammonium chloride significantly reduced it.

Overall, the AC-MnO_2 nanocomposite exhibits strong potential for wastewater treatment applications due to its high adsorption capacity, thermal stability, and effective pollutant removal. These findings highlight its suitability for large-scale environmental remediation, particularly in the removal of organic contaminants. Future studies should focus on optimizing the synthesis process, evaluating reusability, and exploring real wastewater applications to further establish its practical viability.

V. REFERENCE

[1] Slama, H. B., Chenari Bouket, A., Pourhassan, Z., Alenezi, F. N., Silini, A., Cherif-Silini, H., ... & Belbahri, L. (2021). Diversity of synthetic dyes from textile industries, discharge impacts and treatment methods. Applied Sciences, 11(14), 6255.

[2] Ali, H., Khan, E., & Ilahi, I. (2019). Environmental chemistry and ecotoxicology of hazardous heavy metals: environmental persistence, toxicity, and bioaccumulation. Journal of chemistry, 2019(1), 6730305.

[3] Duraisamy, P., Gurusamy, K., & Ganeshan, D. K. (2024). Degradation of reactive blue dye under UV irradation using iron based nanocomposites. Zeitschrift für Physikalische Chemie, (0).

[4] Kavitha, G., Subhapriya, P., Dhanapal, V., Dineshkumar, G., & Venkateswaran, V. (2021). Dye removal kinetics and adsorption studies of activated carbon derived from the stems of Phyllanthus reticulatus. Materials Today: Proceedings, 45, 7934-7938.

[5] Parimaladevi, P., & Venkateswaran, V. (2011). Kinetics, thermodynamics and isotherm modeling of adsorption of triphenylmethane dyes (Methyl violet, Malachite green and Magenta II) on to fruit waste.

[6] Gopalswami, P. M., Ponnusamy, S., Sivakumar, N., & Ilamparithi, A. (2010). Methylene Blue Adsorption onto Low Cost Powdered Activated Carbon from Agricultural Waste- Morus Plant. Nature, Environment and Pollution Technology, 9(2), 317-322

[7] Bai, Y., Pang, Y., Wu, Z., Li, X., Jing, J., Wang, H., & Zhou, Z. (2023). Adsorption of Lead from Water Using MnO2-Modified Red Mud: Performance, Mechanism, and Environmental Risk. Water, 15(24), 4314.

[8] Melhi, S., Alqadami, A. A., Alosaimi, E. H., Ibrahim, G. M., El-Gammal, B., Bedair, M. A., & Elnaggar, E. M. (2024). Effective removal of Malachite Green dye from water using low-cost porous organic polymers: Adsorption kinetics, isotherms, and reusability studies. Water, 16(13), 1869.

[9] Baig, Z., Mamat, O., & Mustapha, M. (2018). Recent progress on the dispersion and the strengthening effect of carbon nanotubes and

graphene-reinforced metal nanocomposites: a review. Critical Reviews in Solid State and Materials Sciences, 43(1), 1-46.

[10] Anastasiadis, S. H., Chrissopoulou, K., Stratakis, E., Kavatzikidou, P., Kaklamani, G., & Ranella, A. (2022). How the physicochemical properties of manufactured nanomaterials affect their performance in dispersion and their applications in biomedicine: a review. Nanomaterials, 12(3), 552.

[11] He, Y., Liu, S., Priest, C., Shi, Q., & Wu, G. (2020). Atomically dispersed metal–nitrogen–carbon catalysts for fuel cells: advances in catalyst design, electrode performance, and durability improvement. Chemical Society Reviews, 49(11), 3484-3524.

[12] Li, Y., Lin, Y., Xu, Z., Wang, B., & Zhu, T. (2019). Oxidation mechanisms of H2S by oxygen and oxygen-containing functional groups on activated carbon. Fuel Processing Technology, 189, 110-119.

[13] Prakalathan, D., Kavitha, G., & Dinesh Kumar, G. (2024). Development of copper oxide-based photocatalysts from copper waste for visible light-driven Congo red degradation. Journal of Materials Science: Materials in Electronics, 35(23), 1561.

[14] Prakalathan, D., Kavitha, G., & Kumar, G. D. (2024). Bioinspired copper oxide nanocomposites: harnessing plant extracts for enhanced photocatalytic performance. Environmental Science and Pollution Research, 31(39), 51415-51430.

[15] Devi, R., Kumar, V., Kumar, S., Bulla, M., Sharma, S., & Sharma, A. (2023). Electrochemical analysis of MnO2 (α, β, and γ)-based electrode for high-performance supercapacitor application. Applied Sciences, 13(13), 7907.

[16] Epling, W. S., Campbell, L. E., Yezerets, A., Currier, N. W., & Parks, J. E. (2004). Overview of the fundamental reactions and degradation mechanisms of NOx storage/reduction catalysts. Catalysis Reviews, 46(2), 163-245.

[17] Walker, G. M., & Weatherley, L. R. (2001). Adsorption of dyes from aqueous solution—the effect of adsorbent pore size distribution and dye aggregation. Chemical Engineering Journal, 83(3), 201-206.

[18] Raji, Z., Karim, A., Karam, A., & Khalloufi, S. (2023, September). Adsorption of heavy metals: mechanisms, kinetics, and applications of various adsorbents in wastewater remediation—a review. In Waste (Vol. 1, No. 3, pp. 775-805). MDPI.

[19] Dieguez-Alonso, A., Funke, A., Anca-Couce, A., Rombolà, A. G., Ojeda, G., Bachmann, J., & Behrendt, F. (2018). Towards biochar and hydrochar engineering—Influence of process conditions on surface physical and chemical properties, thermal stability, nutrient availability, toxicity and wettability. Energies, 11(3), 496

[20] Santhi, M, Kumar P.E. (2015). Adsorption of Rhodamine B from an aqueous solution: Kinetic, Equilibrium and Thermodynamic studies. IJIRST (Volume 4, issue 2).